Physica C 185–189 (1991) 65–71
North-Holland

PHYSICA C

RAMAN SCATTERING IN HIGH-T_c SUPERCONDUCTORS

Manuel CARDONA

Max-Planck-Institut für Festkörperforschung, Heisenbergstr. 1, 7000 Stuttgart 80, Federal Republic of Germany

The use of Raman Spectroscopy for the investigation and characterization of high T_c superconductors is reviewed. A parallel is drawn with some of the effects observed for conventional heavily doped semiconductors. Recent advances are discussed.

1. INTRODUCTION

Raman spectroscopy gained a prominent role in the investigation of high T_c superconductors (high T_c SC's) shortly after their discovery.[1,2] The initial work focussed on phonon eigenvectors,[3] and frequencies and their use for characterizing isotopic substitution.[1] Investigation of phonon anomalies at T_c followed.[4,5] The symmetry properties of B_{1g} phonons of Y-123 at $\sim$340 cm^{-1} were used to identify single domain single crystals.[5] An electronic scattering background, in which a gap opens below T_c, was also early discovered.[5-9] This background was shown to interfere coherently with the phonons, giving rise to Fano-type asymmetric Raman lineshapes.[5] Scattering by two magnons was also early identified in the insulating modifications of high T_c SC's.[10,11]

Recently, absolute scattering efficiencies I_S of Y-123 have been measured and compared favorably with results of LMTO-LDA "ab initio" calculations of the Raman tensor.[12] These results have yielded quantitative information on electron-phonon coupling constants which can also be obtained from the changes in the real[13] and imaginary[14] parts of phonon self-energies (SE) at T_c. For the Raman (and also ir) phonons the electron-phonon coupling constants λ are, at most, one-half of those required to explain T_c's higher than 77 K. These measurements also yield plausible values of the gap ($2\Delta \simeq 5kT_c$) and suggest the presence of more than one gap or a distribution of gaps around the Fermi surface (Y-124, Ref. 15). This can also be inferred from the electronic scattering background.[15] Raman scattering also shows rather normal λ's for the apical oxygen vibrations,[16] a fact which speaks against a dominant role in the high-T_c mechanism. Anomalies in I_S at T_c have also been observed in Y-124[15] and Y-123[17] and attributed to resonant scattering across the superconducting gap. Recently a controversy has arisen about whether in Y-123 the B_{1g} phonons (340 cm^{-1}) sharpen[18,19] or broaden[14] below T_c. This controversy has been solved: sharpening below T_c only happens in samples with strong substitutional doping into the Cu sites.[20]

Scattering by strong coupled phonon-f-electron excitations (of the Nd-ion) has been reported in Nd-123.[21,22] The dependence on temperature of the doublet observed has been related to occupation statistics of the f-electron crystal field levels. Another recent development is the observation of ir-active (Raman forbidden) LO modes in the Raman spectra of $YBa_2Cu_3O_6$ under strongly resonant conditions. They are believed to be "quadrupole allowed" by the strong Fröhlich interaction which accompanies LO phonons.

Several reviews of Raman scattering in high-T_c SC's have appeared.[23-28]

2. ELECTRONIC SCATTERING

Raman scattering by free carriers has been extensively studied in heavily doped semiconductors.[29-32] Free electrons couple to the scattering Hamiltonian through the $\vec{A}\cdot\vec{p}$ term ($\vec{A} = \vec{A}_L + \vec{A}_S$, the sum of the incident and scattered vector potentials) in second order perturbation theory and the A^2 term in first order. Away from resonances, and using the $\vec{k}\cdot\vec{p}$ expression for the free carrier effective mass, the scattering Hamiltonian becomes[29]

$$\vec{A}_L \cdot \frac{1}{\overleftrightarrow{m}} \cdot \vec{A}_S \tag{1}$$

where $\overleftrightarrow{m}$ is the mass tensor of the carriers. If all these carriers have the same $\overleftrightarrow{m}$ Eq. (1) behaves as a longitudinal perturbation inducing a charge density wave which is screened by the carriers. This result in the Stokes efficiency for a carrier concentration N per unit solid angle and unit path length:[32]

$$I_S(\Omega,q) = -\left(\frac{\omega_S}{\omega_L}\right)^2 r_0^2 \left(\hat{e}_L \cdot \frac{m_0}{\overleftrightarrow{m}} \cdot \hat{e}_S\right)^2 \cdot (1+n(\Omega)) \cdot \frac{\hbar q^2}{4\pi\epsilon^2} \cdot Im\frac{1}{\varepsilon(\Omega)} d\Omega \tag{2}$$

where $r_0 = \epsilon^2/m_0c^2$ (Thomson radius), $\Omega = \omega_L - \omega_S$ is the Stokes shift $n(\Omega)$ the corresponding Bose-Einstein factor and $\varepsilon(\Omega)$ the dielectric function, including free and bound carrier

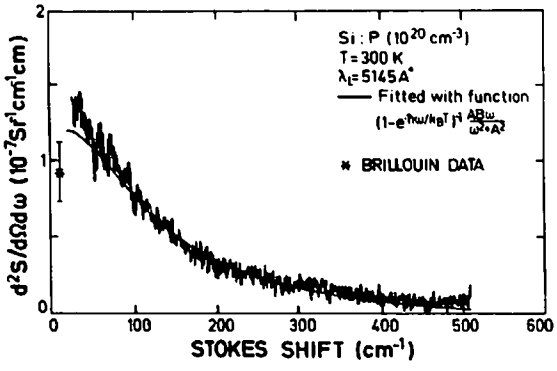

FIGURE 1
Raman scattering by intervalley density fluctuations in n-type silicon fitted with Eq. (3).[30]

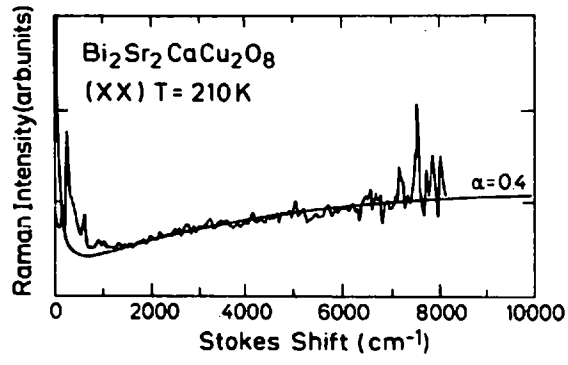

FIGURE 2
Electronic Raman scattering of high-T_c superconductors fitted with Eqs. (3-6).[8,35]

contributions. Equation (2) yields a peak at the screened free carrier plasma frequency Ω_p and a vanishing scattering efficiency for $\Omega \to 0$, $\sim 10^{-5}$ times smaller than the observed one at ~ 100 cm^{-1}.

The smallness of the I_s of Eq. (2) for $\omega \to 0$ is due to screening of the low frequency charge density fluctuations by the free carriers which lowers the coupling to Eq. (1). This screening can be prevented if the density fluctuations have zero charge and nevertheless couple to Eq. (1). This happens in multicomponent carrier systems, e.g., if the various components have different mass tensors. A typical case is that of heavily doped Si (six equivalent valleys along ⟨100⟩) or Ge (four equivalent valleys along ⟨111⟩.[30,31] In these cases there are *intervalley* density fluctuations with zero charge (charge increase in one valley ≡ decrease in another) which are not screened. They scatter the light strongly at low frequencies if the various mass tensors referred to the same set of axes are very different. Such is the case of n-type Si and Ge: for Si, e.g., the mass tensors are uniaxial ($m_{||} = 0.9\, m_0$, $m_\perp = 0.2\, m_0$) and oriented orthogonally to each other for the various valleys. Thus the contributions of these valleys to Eq. (1) do not cancel even if the charge fluctuations do. Scattering by unscreened low frequency density fluctuations results, as shown in Fig. 1.[30] The corresponding Stokes spectra are well represented by (Fig. 1):[30-33]

$$I_S = (1 + n(\Omega)) \frac{B\Omega\tau^{-1}}{\Omega^2 + \tau^{-2}} = (1 + n(\Omega)) \frac{B\Omega\tau^{-1}}{\Omega^2\tau^2 + 1} \qquad (3)$$

where τ^{-1} is the intervalley scattering time and:

$$B = \frac{\hbar e^4}{\pi c^4} \frac{dN}{dE_F} \left\langle \left[\hat{e}_L \cdot \left(\frac{1}{\overleftrightarrow{m}} - \left\langle \frac{1}{\overleftrightarrow{m}} \right\rangle \right) \cdot \hat{e}_S \right]^2 \right\rangle , \qquad (4)$$

⟨...⟩ being the average over all valleys and E_F the Fermi energy. The parameter B is thus determined by the "fluctuations" of $\overleftrightarrow{m}$ over the Fermi surface. Note that these fluctuations are suppressed (and the low frequency scattering eliminated) if all carriers are transferred to a single valley by application of uniaxial stress.[31]

In high-T_c SC's low frequency scattering much stronger than that given by Eq. (2) is observed (Fig. 2).[5-8] It is reasonable to attempt an explanation based on neutral carrier density fluctuations related to mass fluctuations around the Fermi surface.[32] There are, however, two features which resist the fit to Eq. (3):

1. I_S is nearly independent of Ω over a wide frequency range (it increases by less than a factor of 2 from $\simeq$ 0.01 to 1 eV). This is contrary to the strong decrease with increasing Ω required by Eq. (3).

2. I_S is nearly independent of temperature. This is contrary to the dependence required by the Bose-Einstein factor and observed for n-Si and n-Ge.[30,31]

One can try to modify Eq. (3) in a phenomenological way so as to reproduce these features.[34] A microscopic derivation of this modification, based on the existence of large nesting parts of the Fermi surface, has been given.[35] It leads to a replacement of τ^{-1} in Eq. (3) by the frequency and temperature dependent τ:

$$\tau^{-1} = \alpha \cdot Max\, [|\omega| + \beta' T] \qquad (5)$$

where $\alpha \approx 0.5$ and $\beta' \approx 3.5$ (T in units of frequency). This τ^{-1} corresponds to an imaginary part of the self-energy (SE) for electron-electron scattering in a "nesting" situation. The

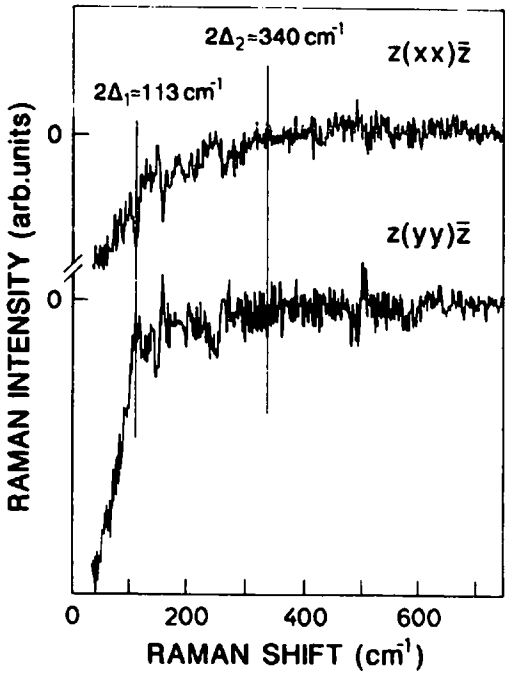

FIGURE 3
Difference in the electronic scattering of $YBa_2Cu_3O_8$ above and below T_c for two different polarization configurations.[22] These data suggest the presence of two energy gaps.

corresponding real part leads to a renormalization of Ω^2 in the denominator of Eq. (3) which must be multiplied by a frequency and temperature dependent effective mass:

$$\frac{m^*(\omega,T)}{m_0} = 1 + \frac{2\alpha}{\pi}\ell n\frac{\omega_c}{Max(\beta T,|\Omega|)} \qquad (6)$$

with ω_c a cutoff $\approx$ 1 eV. Figure 2 shows a fit with Eqs. (5,6) to data of Staufer et al.[8] using α as a fitting parameter. The fit above 800 cm^{-1} is excellent. It is also good between 200 - 800 cm^{-1} if one removes the phonon structures. The divergence of the theory below $\approx$ 200 cm^{-1}, not observed experimentally, may be an artifact of the calculation. It would be of interest to calculate B from the mass fluctuation around the Fermi surface for a realistic band structure, to estimate from it with Eqs. (3 - 6) the absolute I_S, and to compare it with experiments.

The flat electronic continuum of the type of Fig. 2 opens a gap below T_c which, as shown in Fig. 3 for $YBa_2Cu_4O_8$, is not sharp. BCS theory for spherical Fermi surfaces requires a sharp gap $2\Delta \simeq 3.5kT_c$ with zero scattered intensity below 2Δ. It is hard to decide experimentally whether inelastic scattering is present all the way down to $\Omega = 0$ or a sharp cutoff takes place. Fano interference of the vibrations which correspond to the 115 cm^{-1} phonon of $YBa_2Cu_3O_7$

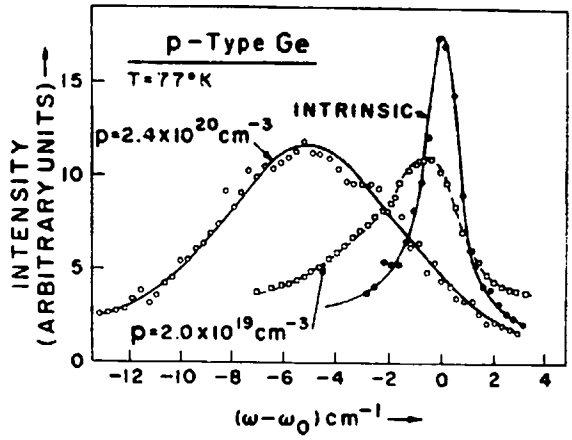

FIGURE 4
Raman spectra of intrinsic and heavily doped p-type Ge showing a broadening and softening due to electron-phonon interaction.[38]

below T_c has been reported in Ref. 36. It indicates that at this frequency some coherent continuum I_S is still available, in agreement with Fig. 3. It is hard to decide, however, whether the universally observed, "soft gap" ("pseudogap") is an intrinsic property of the high T_c SC's or is rather related to material defects or the presence of the surface. The fact that it is observed by many workers and for different samples may favor the intrinsic nature. In any case, Fig. 3 gives different values 2Δ ($2\Delta_1$ and $2\Delta_2$) for xx and yy polarizations, averaging roughly to the BCS value of 3.5 kT_c!. This suggests variations of 2Δ over the Fermi surface with stable points at $2\Delta_2$ and $2\Delta_1$.[37]

3. PHONON ANOMALIES

Effects of the electron-phonon interaction can be directly observed in the Raman spectra of phonons by doping conventional semiconductors. Results obtained for p-type Ge[38] are shown in Fig. 4. The width of the phonon of the intrinsic material, produced by anharmonic decay into two or more phonons, increases upon doping with Ga while its frequency decreases. This is interpreted as due to the SE of the phonons interacting with the holes in the valence band. The real part of this SE is responsible for the phonon softening while its imaginary part produces the broadening. The latter is only non-zero when *real* electron (or hole) transitions can take place at the phonon frequency while the former, a softening, implies that more virtual transitions can take place above the phonon frequency than below.

Similar effects exist in metals but it is not easy to dis-

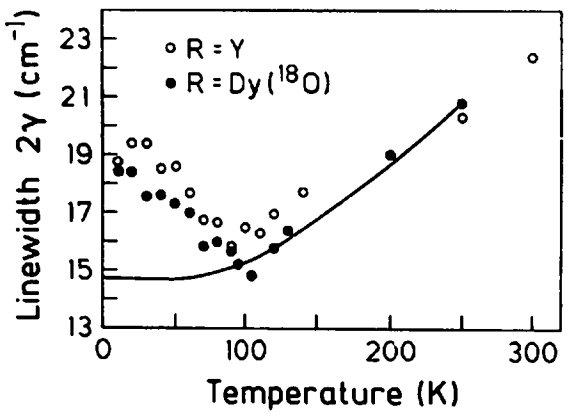

FIGURE 5
Linewidth of the Raman c-stretching mode of the O_{IV} (apical) oxygen of $YBa_2Cu_3{}^{16}O_7$ and $DyBa_2Cu_3{}^{18}O_7$ showing the self-energy effect for $T < T_c$.[16]

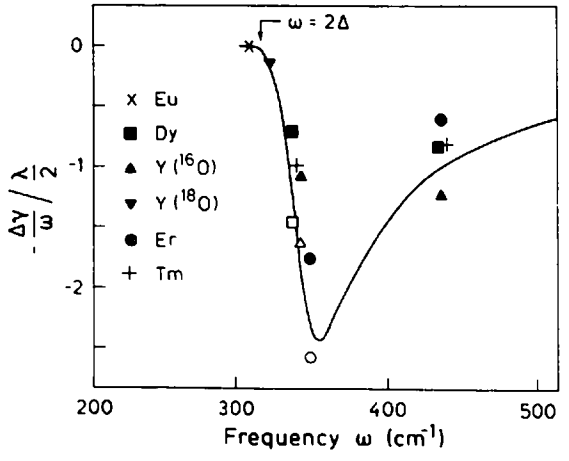

FIGURE 6
Linewidths (normalized to the calculated coupling constant λ) of several 123 SC's versus phonon frequency.[14]

entangle them from elastic backgrounds because of the impossibility of changing the carrier density. In high-T_c SC's changes in the real and imaginary parts of phonon SE's can be observed through the SC transition.[2,3,14-19] The real part of the SE reflects itself in a softening or hardening below T_c, depending on whether the phonon lies below or above the gap. In the former case a sharpening occurs as *real* electronic excitations available for the decay of the phonon are removed below T_c. In the latter, the density of such excitations increases at $\omega = \Omega$ and so do the phonon widths.

Figure 5 shows the *increase* in the linewidth found below T_c for the apical oxygen phonon (vibrations of O_{IV} along c) of two 123-materials. Above T_c the standard anharmonic broadening, fitted with the statistical factor $A(1+2n(\Omega/2))$, is shown. That *increase* indicates that a gap exists at or below those vibrational frequencies, i.e. $\lesssim 480$ cm^{-1}.

A detailed analysis of the temperature dependence of the line width is shown in Fig. 6 for the phonons which correspond to vibrations along c of the oxygens in the CuO_2 planes of many 123-materials. Two such Raman active phonons exist, a fully symmetric one at ~ 440 cm^{-1} and another at ~ 340 cm^{-1} with B_{1g} tetragonal symmetry. The fit of these data to theory[39] yields $2\Delta/kT_c \simeq 5.0$ and for the electron phonon coupling constant $\lambda \simeq 0.5$ (provided *all* phonons couple with the same strength.[14]). The broadenings below T_c in Fig. 6 have been contested in Refs. 18,19. The reason seems to be that the samples in[18,19] contained substitutional impurities (Au, Th) which strongly affect the anisotropy of the gaps and change broadenings of the 340 cm^{-1} mode into sharpenings (Fig. 7).[20]

Not only the SE's exhibit anomalous behavior at T_c but

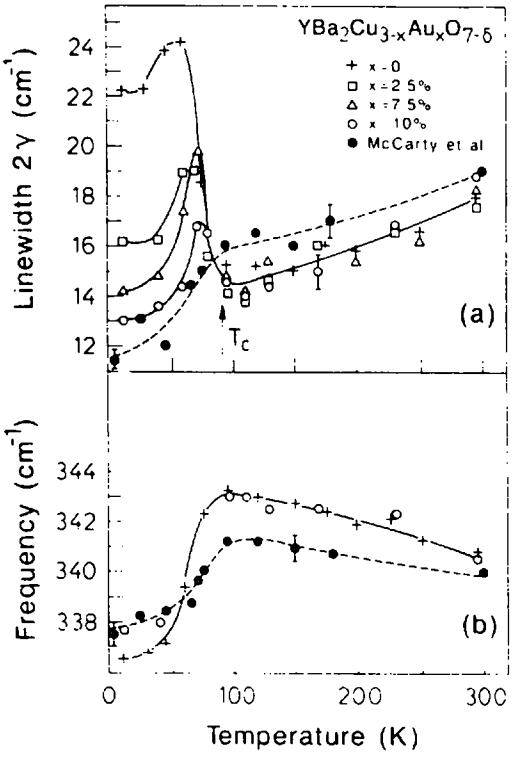

FIGURE 7
Linewidth 2γ and frequency shifts with T of the B_{1g} (tetragonal notation) phonons of $YBa_2Cu_{3-x}Au_xO_7$ for several values of x. With increasing x the effect on γ evolves from a broadening to a sharpening below T_c.[20]

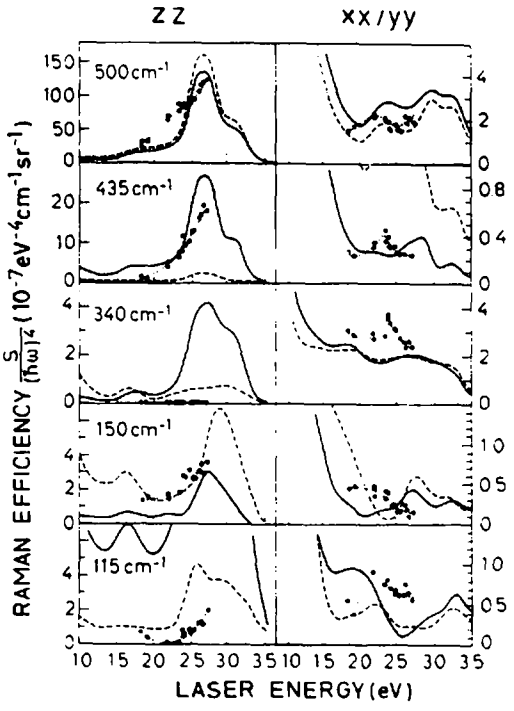

FIGURE 8
Resonance profiles of several Raman phonons in absolute Raman efficiency units, compared with LMTO calculations (also absolute!). The dashed lines represent calculation for unmixed ionic motion modes while the solid lines represent fits with mode admixture. Note that 435 mode derives its strength from the mode admixture while the 115 (Ba-like) and 150 cm^{-1} (Cu-like) modes seem to be unmixed.[12]

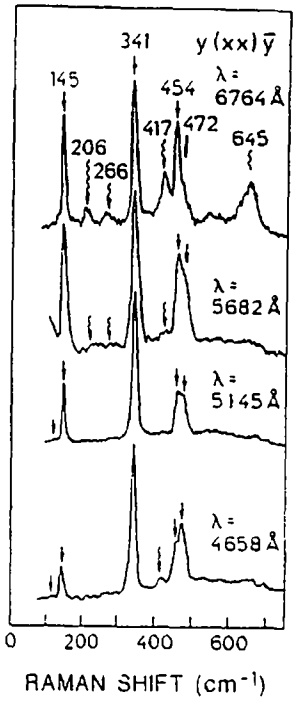

FIGURE 9
Resonant Raman spectra of $YBa_2Cu_3O_6$ showing Raman forbidden, ir-active LO modes (wavy arrows).[22]

also the I_S's: a sharp increase is usually found below T_c (sometimes a decrease, depending on phonon and ω_L).[17,22] This has also been interpreted as due to a resonance of the phonon frequency with the gap.[17,22]

4. RESONANT RAMAN PHENOMENA

I_S depends strongly on laser frequency (Fig. 8)[21,40] and exhibits structures characteristic of resonances of ω_L and/or ω_S with strong interband transitions. The resonance profiles of Fig. 8 were calculated from *ab initio* LMTO band structures by evaluating the dielectric function $\varepsilon(\omega)$ and its derivative with respect to the phonon coordinate. The agreement obtained between calculated and measured I_S *in absolute units* is remarkable. To the best of our knowledge this is the first material with a unit cell of more than 2 atoms for which such theoretical work has been performed. The results give a lot of confidence in electron-phonon coupling constants obtained from band structure calculations. From this work information about the phonon eigenvectors can be obtained. It was shown[12] that best agreement with the measured Raman profile is found for nearly pure Ba-modes (solid line in Fig. 8) while the profiles of the A_{1g} vibration of the plane oxygen requires admixture of apical oxygens.

Another interesting resonance phenomenon is the appearance of Raman forbidden, ir-allowed phonons near resonance in the non-superconducting modification of the 123-materials ($YBa_2Cu_3O_6$). These modes are shown by wavy arrows in Fig. 9. They are interpreted as quadrupole allowed, induced by the Fröhlich electron-phonon interaction.[41] The observed peaks have been assigned to the LO components of vibrations perpendicular to c (E_u symmetry), since their frequencies agree with ir-reflectivity data.[42] Of the six modes of this symmetry four are seen in Fig. 9. They correspond to vibrations of the yttrium (206 cm^{-1}), OII,III (266 cm^{-1}, OIV (417 cm^{-1}) and OII (645 cm^{-1}).

The reason why no ir-active modes polarized along c (A_{2u}) are observed is attributed to the large effective masses of electronic bands along this direction (the Fröhlich scattering amplitude is proportional to the difference of the inverse effective masses of participating valence and conduction bands along the polarization direction of the phonon[43]).

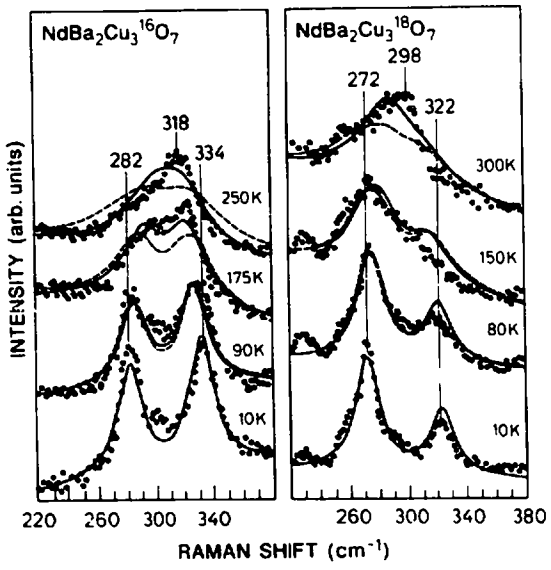

FIGURE 10
Mixed cfe-phonon coupled modes in the Raman spectra of $NdBa_2Cu_3O_7$ (^{16}O and ^{18}O isotopes).[21,22]

5. MIXED PHONON CRYSTAL-FIELD EXCITATIONS

The rare earth ions of high-T_C SC's have, with the exception of La and Y, strongly localized $4f$ electrons whose ionic levels are split by Coulomb interaction into many-electron angular momentum states. These states split further under the action of the rather low symmetry crystal field (e.g. D_{2h} for $NdBa_2Cu_3O_7$, D_{4h} for the O_6 modification). They are at least doubly (Kramers) degenerate if the number of f-electrons is odd, such as for Nd^{3+} ($3f$-electrons). Transitions between the crystal field ground state and excited states (cfe) have been observed by neutron scattering.[44,45] They are usually too weak to be seen in Raman scattering owing to the localized nature of the f-electrons. In some special cases, however, f-electron excitations are nearly degenerate with phonons of the same symmetry. Such is the case of $NdBa_2Cu_3O_{7-\delta}$. A B_{1g} (tetragonal notation) crystal field excitation is nearly degenerate with the B_{1g} phonon, whose frequency lies slightly above that of the cfe for O^{16} and slightly below O^{18}.[21,22] Electron-phonon coupling produces in this case a strong mixing of the B_{1g} electronic and vibronic excitations, a doublet results with nearly equal mixture of both components. Both members of the doublet can thus be seen in the Raman spectra (Fig. 10), with the higher frequency component slightly stronger than the lower one for O^{16} and slightly weaker for O^{18}, as expected. Both components shift by half of the change in the square root of the O-mass when O^{16} is replaced by O^{18}, owing to the fact that each component is only partially an O-vibration. With increasing temperature, the occupation of the crystal field levels changes, most consequential being the decrease of the population of the crystal field ground state. This results in an effective decrease of the coupling between phonons and cf levels[21,41] which is also displayed in Fig. 10.

6. REFERENCES

1. B. Battlog et al., Phys. Rev. Lett **58**, 2333 (1987).
2. R. Liu et al., Solid State Commun **63**, 839 (1987).
3. R. Liu et al., Phys. Rev. B **37**, 7971 (1988).
4. R.M. Mcfarlane et al., Solid State Commun. **63**, 831 (1987).
5. C. Thomsen et al., Phys. Rev. B **37**, 9860 (1988).
6. K.B. Lyons et al., Phys. Rev. B **36**, 5592 (1987).
7. Y.A. Ossipyan et al., Physica C **153 - 155**, 1133 (1988).
8. Staufer et al., Solid State Commun. **75**, 975 (1990), also to be published.
9. S.L. Cooper et al., Phys. Rev. B **37**, 5920 (1988).
10. K.B. Lyons et al., Phys. Rev. Lett. **60**, 732 (1988).
11. S. Sugai et al., Phys. Rev. B **38**, 6436 (1988).
12. E.T. Heyen et al., Phys. Rev. Lett. **65**, 3048 (1991).
13. C. Thomsen et al., Solid State Commun. **75**, 219 (1990).
14. B. Friedl et al., Phys. Rev. Lett. **65**, 915 (1990).
15. E.T. Heyen et al., Phys. Rev. B **41**, 11058 (1990).
16. B. Friedl et al., Solid State Commun. **76**, 1107 (1990).
17. B. Friedl et al., Solid State Commun. **78**, 291 (1991).
18. E. Altendorf et al., Physica C **175**, 47 (1991).
19. K.F. McCarty et al., Phys. Rev. B **43**, 13751 (1991).
20. C. Thomsen et al., Solid State Commun. **78**, 727 (1991).
21. E.T. Heyen et al., Phys. Rev. Lett. **67**, 144 (1991).
22. E.T. Heyen et al., Phys. Rev. B, in press.
23. C. Thomsen and M. Cardona, in *Physical Properties of High Temperature Superconductors I*, ed. by D.M. Ginsberg (World Scientific, Singapore, 1989), p. 409.
24. R. Feile, Physica C **159**, 1 (1989).
25. M. Cardona, Proc. of Int. Conf. on High T_c Superconductivity - ICSC, eds. S.K. Joshi, C.N.R. Rao, S.V. Subramanyam (World Scientific, Singapore, 1990), p. 208.
26. C. Thomsen, in *Light Scattering in Solids VI*, ed. by M. Cardona and G. Güntherodt (Springer Verlag, Heidelberg, 1991), p. 285.
27. J.R. Ferraro and V.A. Maroni, Appl. Spectrosc. **44**, 351 (1990).
28. H. Kuzmany et al., in *Status of High Temperature Superconductivity, Advances in Research and Applications*, Vol. 3, ed. by A. Narlikar (Nova, New York, 1989), p. 299.
29. for a review see G. Abstreiter et al., in *Light Scattering in Solids IV*, M. Cardona and G. Güntherodt, eds. (Springer, Heidelberg, 1984).
30. G. Contreras et al., Phys. Rev. B **32**, 924 (1985).

31. G. Contreras et al., Phys. Rev. B **32**, 930 (1985).

32. M.V. Klein, in *Light Scattering in Solids I*, M. Cardona, ed. (Springer Heidelberg, 1982).

33. A. Zawadowski and M. Cardona, Phys. Rev. B **42**, 10732 (1990).

34. C.M. Varma et al., Phys. Rev. Lett. **63**, 1996 (1989).

35. A. Virostek and J. Ruvalds, to be published.

36. S.L. Cooper et al., Phys. Rev. B **38**, 11934 (1988).

37. R. Comberscot, Phys. Rev. Lett. **67**, 148 (1991).

38. F. Cerdeira and M. Cardona, Phys. Rev. B **5**, 1440 (1972).

39. R. Zeyher and G. Zwicknagl, Z. Phys. B - Condens. Matt. **78**, 175 (1991).

40. M. Boekholt and G. Güntherodt, subm. to Physica C.

41. E.T. Heyen, to be published.

42. M. Bauer et al., subm. to Z. Phys. B (1991) also, Solid State Commun. **72**, 551 (1989).

43. M. Cardona in *Light Scattering in Solids II* (Springer, Heidelberg, 1983), p. 39.

44. P. Allenspach et al., Physica B **156-157**, 854 (1989).

45. G.L. Goodman et al., J. Phys. Cond. Matt. **3**, 49 (1991).